Article

Bicarbonate inhibition of Carbonic Anhydrase mimics hinders catalytic efficiency: Elucidating the mechanism and gaining in-sight towards improving speed and efficiency

Jonathan Rains, Kerry O'Donnelly, Thomas Oliver, Rudiger Woscholski, Nicholas J. Long, and Laura M. C. Barter

ACS Catal., **Just Accepted Manuscript** • DOI: 10.1021/acscatal.8b04077 • Publication Date (Web): 03 Jan 2019

Bicarbonate Inhibition of Carbonic Anhydrase Mimics Hinders Catalytic Efficiency: Elucidating the Mechanism and Gaining Insight Towards Improving Speed and Efficiency

Jonathan G. D. Rains, Kerry O'Donnelly, Thomas Oliver, Rudiger Woscholski*, Nicholas J. Long*, Laura M. C. Barter*

Institute of Chemical Biology, Department of Chemistry, Imperial College, Molecular Science Research Hub, White City Campus, London, W12 0BZ, UK.

*Email: r.woscholski@imperial.ac.uk; n.long@imperial.ac.uk; l.barter@imperial.ac.uk

Abstract. Carbonic Anhydrase (CA) mimics are often studied with a focus on the hydration of CO_2 for atmospheric carbon capture. Consequently, the reverse reaction (dehydration of HCO_3^-) has received minimal attention, so much so, that the rate-limiting step of the dehydration reaction in CA mimics is currently unknown. The rate-limiting step of the hydration reaction is reported to be the bicarbonate-bound intermediate step, and thus is susceptible to product inhibition. It is not, however, clear if this inhibition is a consequence of an increase in the rate of the competing dehydration reaction or resulting from the strong affinity of bicarbonate to the mimic. To address this, insight into the dehydration reaction kinetics is needed. We therefore report the most comprehensive study of a CA mimic to date. The dehydration profile of the fastest small-molecule CA mimic, ZnL1S, was characterised and consequently evidence for the rate-limiting step for the dehydration reaction was seen to be the bicarbonate-bound intermediate step, much like the hydration reaction. This experimental validation of the rate-limiting step was achieved through a variety of methods including NMR experiments and the effect of inhibitors, substrate concentration and metal centre on activity. With this understanding, an improvement in the favourability of the rate-limiting step was achieved resulting in decreased bicarbonate inhibition. Thus, an increase in the mimic's k_{cat} for both reactions was observed, resulting in the largest rate constants of any small-molecule CA mimic reported to date (28,093 and 579 M^{-1} s^{-1} for hydration and dehydration respectively). Enzyme-like k_{cat} / k_m values were obtained for ZnL1S (5.9 x 10^5 M^{-1} s^{-1} for CO_2 hydration) and notably there is only a difference of 2.5 orders of magnitude with the enzyme, the closest of any CA mimic reported in the literature. The results from this work can be applied to the development and improvement of future and existing mimics towards attaining increased activities.

Keywords. Carbonic Anhydrase, Biomimetic, HCO_3^- dehydration, CO_2 hydration, rate-limiting step, stopped-flow

Introduction. The capture of CO_2 produced during industrial processes, or directly from the atmosphere, are important processes and have received significant attention in order to reduce the impact of climate change resulting from increased atmospheric CO_2.[1-3] Frequently, synthetic mimics of the enzyme Carbonic Anhydrase (CA),[4-6] which catalyse the reversible reaction between carbon dioxide hydration and bicarbonate dehydration, are investigated as CO_2 capture agents, for storage or other uses.[3, 7-15] Most synthetic CA mimics replicate the active site of the α class of mammalian CA's and thus are composed of a hetero-macrocycle scaffold coordinating zinc,[16-19] and are often designed for use in organic solvents.[9] There are reports of CA mimics that are catalytically active in aqueous solutions at similar rates to those that work only in organic solvents, albeit with rates around 4-5 orders of magnitude slower than the natural enzyme.[18, 20-23]

An example of a CA mimic, ZnL1S (Chart 1), that works in aqueous environments and possesses one of the fastest rates of CO_2 hydration to date.[24] It coordinates a zinc ion through a scaffold containing three histidine-like imidazole ligands and a water molecule. Additionally, the authors state that the ligand generates a hydrophobic pocket within the structure, facilitating the direction of CO_2 approach to the reactive zinc centre, thereby overcoming the activation barrier of CO_2 hydration and thus increasing hydration rates.[24] While the CA mimics and the natural CA enzyme have the same catalytic mechanism (Scheme 1) [4, 25], their kinetics differ significantly.

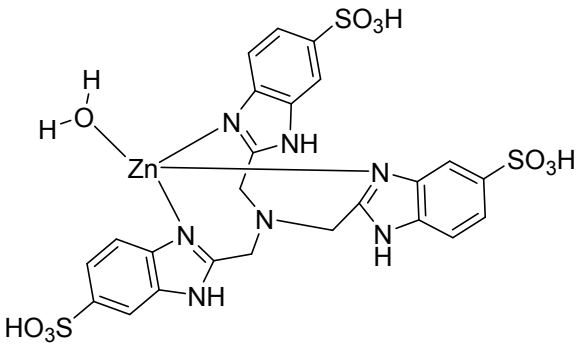

Chart 1. ZnL1S, a water-soluble small-molecule CA mimic.

The rate-limiting step of the natural enzyme is the deprotonation of the bound water molecule, which, due to the shuttling of protons, is essentially diffusion limited (Step 1 in Scheme 1 highlighted in blue).[26] For this reason, it has one of the highest known enzymatic catalytic activities, with a rate of CO_2 hydration of ~10^6 molecules per second per enzyme.[4, 25]. In contrast, the rate-limiting

step in the hydration catalytic cycle of CA mimics is the bicarbonate release step (Step 4 in Scheme 1 highlighted in red). This is due to the favourable low energy of the bidentate bicarbonate-bound intermediate, and has been observed in mimics using macrocycle ligands.[9-11, 17, 20, 27] The consequence of the CA mimics' rate-limiting step is that they are susceptible to product inhibition by the formed bicarbonate ion, thus decreasing the hydration catalytic rates. [9-11, 17, 20, 27] In contrast, the surrounding amino acid environment in the natural enzyme's active site likely facilitates bicarbonate release and an easier water approach by forming an extensive hydrogen bonding network.[28-30]

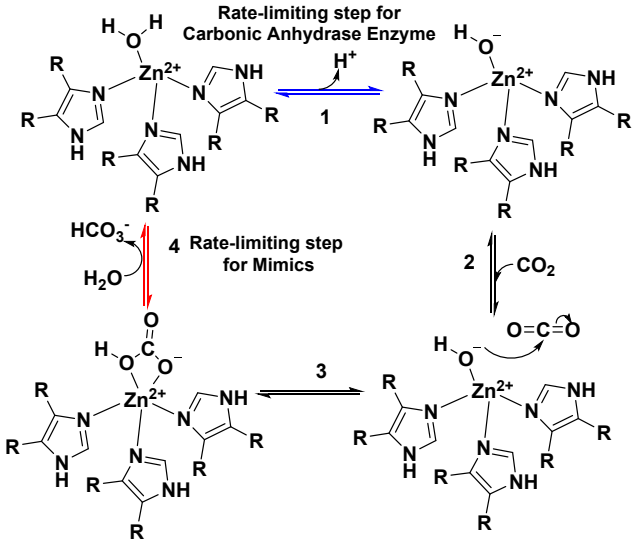

Scheme 1. The mechanism of Carbonic Anhydrase and its mimics. Step 1 (Blue): Deprotonation of a zinc-bound water to generate $(His)_3$-Zn-OH^-. Step 2: Nucleophilic attack of CO_2. Step 3: Bicarbonate-bound intermediate formed. Step 4 (Red): Displacement of bicarbonate by water to generate the complex initial state. The R groups on the zinc-coordinating imidazole's represent either an attached benzene moiety to form benzimidazole, like in ZnL1S,[24] or as part of a histidine amino acid, as is the case for the active site of the mammalian α-Carbonic Anhydrase.[4]

For the application of industrial scale CO_2 capture from the atmosphere, efficient and environment-friendly catalysts are needed. [3, 7-15] To generate the next generation of CA mimics the intrinsic product inhibition of the hydration reaction needs to be understood before this obstacle can be overcome. Given the reversibility of the mechanism, it is not clear if the product inhibition is a consequence of an increase in the dehydration reaction, favoured by the presence of the bicarbonate complex, or caused by a strong affinity of bicarbonate to the CA mimetic. To address this more insight into the dehydration reaction kinetics is needed. With the emphasis of research focusing on CO_2 hydration catalysts, [3, 7-15] there is however a huge void of understanding concerning the dehydration of HCO_3^- by these CA mimics and their rate limiting step.[18, 22, 31-37]

Here, we present an extensive characterisation of the often-ignored dehydration reaction for the fastest small-molecule water-compatible CA mimic (ZnL1S). Kinetic measurements using stopped-flow and other relevant techniques were employed, providing the necessary insights to improve the next generation environment-friendly CO_2 capture catalysts. We report the rate-limiting step for the dehydration reaction by a CA mimic for the first time. Furthermore, this study achieves the highest reported activities by a CA mimic. Finally, we show that under specific conditions both the dehydration and hydration reaction activities can be improved significantly beyond what is currently reported. Thus, ZnL1S has the potential to be the fastest mimic of CA known to date. Following the evidence of the bicarbonate inhibition, this work concludes with a comparison between the mimic and the enzyme, including their analysis methodologies, and consequently the true potential of ZnL1S is revealed.

Experimental. Experimental information including instrument details, compound characterisation and reagent sources, are detailed in Supporting Information 1a.

Synthesis of the ligand L1S and its metal complexes. The ligand L1S was synthesised using an adaption of the literature method [38] (detailed in Supporting Information 1b) which resulted in an improved purified yield (92% yield) and reaction time (overnight) from the original synthesis procedure for the ligand and complex by Nakata *et.al.* [24] In brief, 3,4-diaminobenzenesulfonic acid was reacted with nitrilotriacetic acid in a double condensation reaction in ethylene glycol to form the ligand L1S. The complexes (ZnL1S, CuL1S, NiL1S and CoL1S) were synthesised by reacting the ligand L1S with the appropriate hydrated metal perchlorate salt in water and precipitating upon the addition of ethanol. See Supporting Information 1c for synthetic details and characterisation.

Kinetic measurement of CO_2 hydration and HCO_3^- dehydration. The hydration and dehydration rate measurements were undertaken by detecting the associated pH change through the use of an appropriate colorimetric pH indicator via stopped-flow equipment (Applied Photophysics SX-20 Stopped-flow Spectrometer).[39] The pH time-dependence of CO_2 hydration or HCO_3^- dehydration was observed via the absorbance change of a buffered indicator solution in order to measure the change in $V_{hydr/dehydr}$ over a concentration range of catalyst, and to determine the observed rate constant (k_{obs}) for each reaction.

Following the previously reported procedure,[24] a 0.1 M buffer solution containing 10 x 10^{-5} M indicator, 0.2 M $NaClO_4$ and varying concentrations of the zinc complex (ZnL1S) in water were loaded into one syringe and a CO_2 or HCO_3^- solution in the other. CO_2 saturated solutions (33.8 mM) were prepared by bubbling CO_2 gas through water for 1 hour at 25°C. The saturated solution was diluted appropriately to give the desired concentration of CO_2. HCO_3^- solutions were prepared by dissolving $NaHCO_3$ in water to give the desired concentration of HCO_3^-. The

buffer-indicator pairs were chosen based upon their similar pKa's, and the pH of the buffer-indicator solution was adjusted to match these pKa's to maximize sensitivity to pH change (Table S1).

Upon mixing of the two syringes, the change in absorbance over time was measured at 25°C. For each buffer solution employed over the tested pH range, the buffer factor (change in absorbance vs concentration of HCl/ NaOH) and linearity of CO_2 and HCO_3^- (change in absorbance vs concentration of CO_2/ HCO_3^-) were determined as controls (Figure S5 and S6 for the buffer factor and substrate linearity respectively). Based upon the linearity of the response between CO_2 or HCO_3^- concentration and change in absorbance, appropriate concentrations of CO_2 or HCO_3^- were chosen within the linear range for the subsequent complex runs. At each concentration of complex, the V_{hydr} (rate of hydration) and V_{dehyd} (rate of dehydration) was measured and k_{obs} (observed rate constant) was calculated as per the procedure of Nakata *et al.*[24] It is of note that not all of the observed rate constants for hydration were obtained from a linear correlation (R^2>0.9) between catalyst concentration and rate. In contrast, all dehydration k_{obs} were obtained from linear plots. k_{cat} (catalytic rate constant) was calculated as the pH independent catalyst rate constant as per Nakata *et al.* and Koziol *et al.* for the hydration reaction ($k_{cat} = k_{obs}$ x (([H^+]/Ka) + 1)) ,[20, 24] and Sun *et al.* for the dehydration reaction (k_{cat} = (k_{obs} x ([H^+] + Ka)) / [H^+]).[35] Each run of 3 repeats was undertaken 3 times and the average taken, to give N = 9.

NMR studies of bicarbonate-bound intermediate. Studies of the catalysis mechanism of reaction were carried out and monitored via ^{1}H and ^{13}C NMR at 25°C. For the dehydration reaction using ^{13}C-labelled sodium bicarbonate, three solutions were prepared in NMR tubes; 0.01 M complex (ZnL1S), 0.01 M substrate ($NaHCO_3$) and 0.01 M complex mixed with 0.01 M substrate (ZnL1S + $NaHCO_3$). All three solutions were made up twice, once in deuterated DMSO and once in D_2O (both H_2O-free). The solutions were then analysed by NMR. For the hydration reaction using ^{13}C-labelled CO_2, 1 atm (approximately 0.2 mmol) of $^{13}CO_2$ was added to the appropriate Young's tap NMR tubes using a Toepler pump. As before, the three solutions (ZnL1S complex, CO_2 substrate and ZnL1S complex + CO_2 substrate) were made up twice, once in deuterated DMSO and once in D_2O. The subsequent hydration NMR studies were carried out in D_2O with increasing concentrations of $NaHCO_3$ or ^{13}C labelled $NaHCO_3$ (0.001 M, 0.01 M & 0.1 M) and one concentration of $NaNO_3$ (0.01 M) in the appropriate Young's tap NMR tube containing 0.01 M ZnL1S and 1 atm (approximately 0.2 mmol) $^{13}CO_2$. The solutions were all analysed using a Bruker AMX-400 spectrometer at room temperature.

4-Nitrophenyl acetate hydrolysis assay. The hydrolysis of 4-nitrophenyl acetate to 4-nitrophenolate with the addition of ZnL1S was monitored following the previously reported procedure at 25°C.[40] 50 µl of 1 mM ZnL1S (100 mM TAPS pH 8.2, 200 mM $NaClO_4$) was incubated with varying concentrations of CO_2 or $NaHCO_3$ for 5 minutes in a 96-well microplate. 50 µl of 5 mM 4-nitrophenyl acetate was added to start the reaction. The formation of 4-nitrophenolate was monitored at 348 nm in a Thermo Scientific Varioskan Flash Multimode microplate reader for 2000 seconds. Final concentrations of CO_2 or HCO_3^- in 100 µl were 0 mM, 1.69 mM, 3.38 mM, 6.76 mM, 10.14 mM, 13.52 mM and 16.9 mM. Δ absorbance / min was calculated by subtracting the final absorbance from the starting absorbance and then dividing by the rate constant as calculated from the slope of time against absorbance.

Results and Discussion.

Synthesis and Catalytic Validation of ZnL1S. In this study, the previously reported fastest water-compatible small-molecule CA active site mimic ZnL1S, which uses the nitrilotris(2-benzimidazolylmethyl) ligand,[24] was successfully synthesised and its catalytic properties validated. The first step in the generation of the water-soluble metal complex ZnL1S was the synthesis of the ligand, L1S, as described previously in the experimental and in more detail in the Supporting Information (Scheme S1 and Figures S7 and S8). The L1S ligand was then complexed with zinc as described in the experimental. The synthesized ligand and the resulting complex, ZnL1S, were fully characterised by ^{1}H and ^{13}C NMR spectroscopy, mass spectrometry and elemental analysis (Scheme S2 and Figure S9). It is of note that due to the new ligand synthesis procedure, as described in the methods, only the 665 isomer was seen in the product (whereas Nakata *et al.* saw the 665 and 666 isomers [24])which is of a benefit for characterisation and subsequent studies. See Chart S1 for structures.

Previously, CO_2 hydration rates of ZnL1S were measured at temperatures of 5, 10 and 15°C. This data was used to extrapolate rates to 25°C, resulting in a predicted catalytic rate constant of 10,000 M^{-1} s^{-1}.[24] While this predicted rate constant makes ZnL1S the fastest reported hydration small-molecule CA mimic, there is clearly a lack of experimental data at "greener" ambient temperatures, i.e. at 25°C, which would require no heating or cooling inputs during the industrial process. Interestingly, the dehydration properties of ZnL1S have been previously studied at 25°C at pH 6 (k_{cat} of 363 M^{-1} s^{-1}),[37] however only using the less sensitive and less accurate weight loss method, and not the stopped-flow method more commonly reported for the hydration reaction.

To address this, both the CO_2 hydration and HCO_3^- dehydration of ZnL1S were analysed using the stopped-flow method up to 25°C. (Table S2). We found a rate constant for CO_2 hydration of 9358 M^{-1} s^{-1} for ZnL1S at 25°C, which is within reasonable agreement with the previously predicted value (10,000 M^{-1} s^{-1}).[24] For the HCO_3^- dehydration reaction, we determined a catalytic rate constant of 103.1 M^{-1} s^{-1} at 25°C, making ZnL1S the fastest small-molecule CA mimics for HCO_3^- dehydration reported to date. It should be noted that the dehydration rate constant for ZnL1S had been previously measured using the less accurate weight loss method, and a catalytic rate constant of 363 M^{-1} s^{-1} was found.[37] This variation in

measured values can be accounted for by the difference in accuracy of the methodology employed. It is of note that there was agreement with the literature for the hydration reaction as the same stopped-flow methodology was utilized. In conclusion, ZnL1S is confirmed to be the fastest water-soluble small-molecule CA mimic for both hydration and dehydration reactions.

Effect of Substrate Concentration and pH on ZnL1S CA Activity. To investigate the rate-limiting step of the dehydration reaction, the kinetic properties of ZnL1S for both reactions (dehydration, and for comparison hydration) were studied across multiple pH's and substrate concentrations.

The dehydration reaction showed a linear decrease in rate with increasing HCO_3^- concentration (Figure S11). Plotting the ratio V_{dehyd} / HCO_3^- against catalyst concentration generated linear trends for all HCO_3^- concentrations. Additionally, there was an inhibitive effect with increasing substrate concentration and the effect was greater at the higher concentration of catalyst (as seen by the greater slope at higher mimic concentrations in Figure S11). Furthermore, the k_{obs} decreased linearly with increasing substrate concentration (Figure 1 E-G).

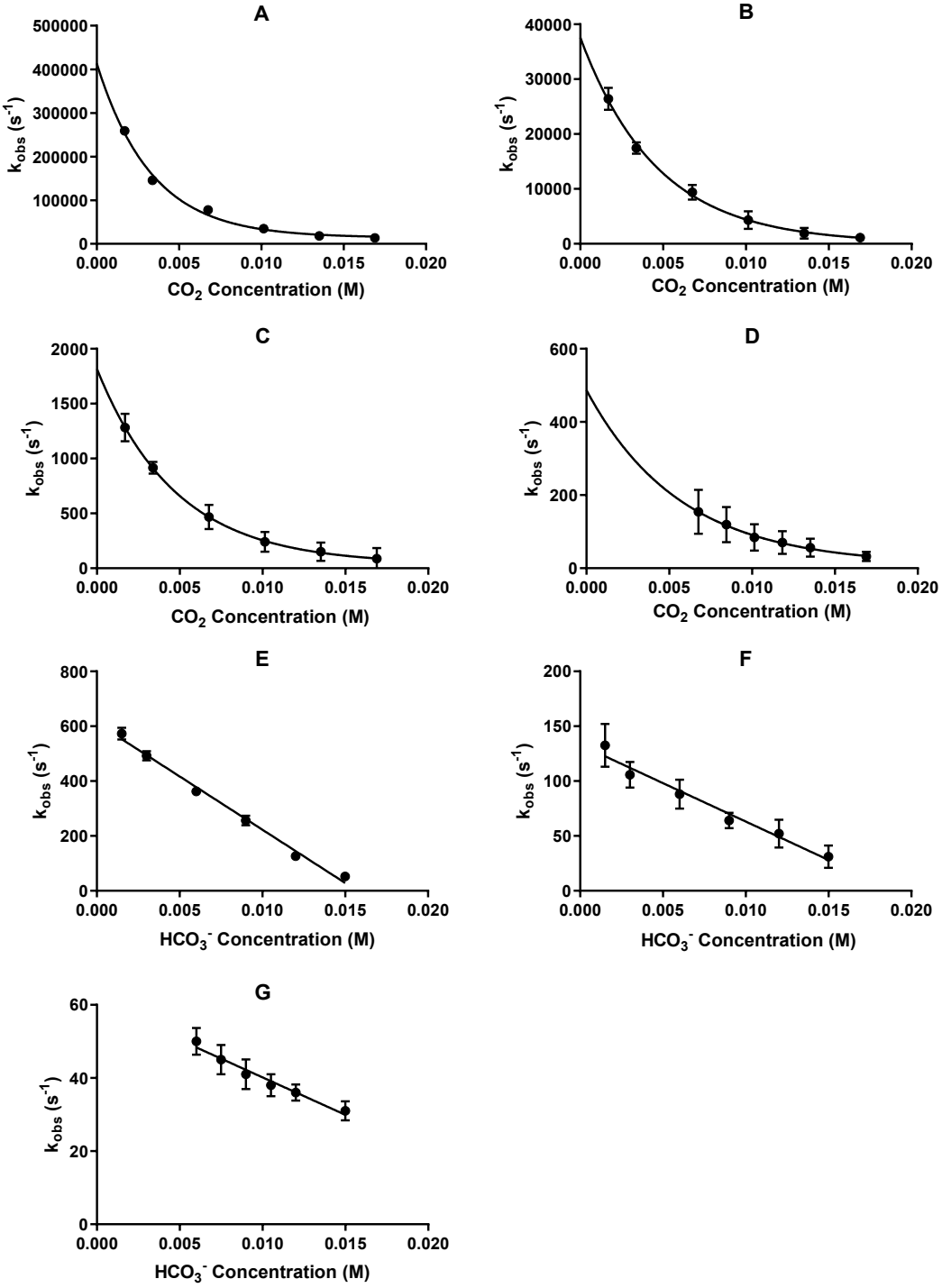

Figure 1. The non-linear relationship between the k_{obs} of ZnL1S for CO_2 hydration across the studied pH range (**A-D** pH 10.8, 9.5, 8.2 and 7.4 respectively). At pH 7.4 (**D**), concentrations below 0.00676 M CO_2 were below the limit of detection. The linear relationship between k_{obs} of ZnL1S (0.5, 5 and 50 μM ZnL1S) for HCO_3^- dehydration across the studied pH range (**E-G** pH 6.3, 7.4 and 8.2 respectively). At pH 8.2 (**G**), concentrations below 0.005 M HCO_3^- were below the limit of detection. k_{obs} data is the slopes of the data shown in Figure S10 B, D, F and H and Figure S11 B, D and F using 0.5, 5 and 50 μM ZnL1S (and 500 μM ZnL1S at pH 10.8). Error bars are the error associated with the fit to generate k_{obs}

Table 1. k_{obs} values for the hydration of CO_2 and the dehydration of HCO_3^- by ZnL1S across the studied range of pH values and substrate concentrations.

		pH 6.3 k_{obs} (M^{-1} s^{-1})	pH 7.4 k_{obs} (M^{-1} s^{-1})	pH 8.2 k_{obs} (M^{-1} s^{-1})	pH 9.5 k_{obs} (M^{-1} s^{-1})	pH 10.8 k_{obs} (M^{-1} s^{-1})
Hydration $[CO_2]$ (M)	**0.00169**	Below LOD	Below LOD	1282 ± 125.4	26426 ± 2021	258753 ± 4242
	0.00338			916.1 ± 54.16	17465 ± 1044	145698 ± 2563
	0.00676		154.10 ± 60.48 *	466.6 ± 110.1 *	9397 ± 1358	77679 ± 2969
	0.00845		119.30 ± 48.41*	Not Measured	Not Measured	Not Measured
	0.01014		84.48 ± 36.36 *	239.8 ± 90.00 *	4333 ± 1609 *	34739 ± 3224
	0.01183		70.26 ± 30.59*	Not Measured	Not Measured	Not Measured
	0.01352		56.05 ± 24.79 *	150.5 ± 83.00 *	1911 ± 962.5 *	18157 ± 1546
	0.0169		31.92 ± 12.84 *	86.88 ± 97.82*	1105 ± 769.7 *	13346 ± 1545
Dehydration $[HCO_3^-]$ (M)	**0.0015**	572.7 ± 21.39	132.5 ± 9.56	Below LOD	Below LOD	Below LOD
	0.003	491.6 ± 16.89	105.7 ± 11.57			
	0.006	361.9 ± 15.77	88.02 ± 13.25	49.53 ± 3.689		
	0.0075	Not Measured	Not Measured	45.36 ± 3.865		
	0.009	255.6 ± 17.97	63.53 ± 7.114	40.77 ± 4.061		
	0.0105	Not Measured	Not Measured	38.22 ± 3.140		
	0.012	126.1 ± 7.998	51.90 ± 12.82	35.67 ± 2.245		
	0.015	51.88 ± 0.7247	30.53 ± 10.26	31.14 ± 2.601		

The data is the average of three repeats. * indicates that the plot of $V/[CO_2]$ vs [ZnL1S] for that [substrate] had an $R^2<0.9$. LOD= limit of detection. k_{obs} data is the slopes of the data shown in Figure S10 B, D, F and H and Figure S11 B, D and F using 0.5, 5 and 50 μM ZnL1S (and 500 μM ZnL1S at pH 10.8). Extra substrate concentrations were studied for pH 7.4 Hydration and pH 8.2 Dehydration to compensate for the loss of data points at lower substrate concentrations.

For the hydration reaction, there was an exponential decrease in rate with increasing CO_2 concentration, across all conditions (Figure S10). The inhibitory effect was greater at higher concentrations of catalyst (as seen by the greater slope at higher mimic concentrations in Figure S10). Additionally, the catalyst's observed rate constant (k_{obs}) decreased exponentially with increasing CO_2 concentration (Figure 1 A-D). Upon plotting of V_{hyd}/CO_2 against catalyst concentration, the linearity of this trend improved with decreasing concentrations of CO_2, indicating less bicarbonate inhibition (i.e. the R^2 value of the linear plot increased towards 1, Table S3). The catalysts appear more inhibited by bicarbonate with increasing catalyst concentration, due to the subsequent increased bicarbonate produced. Thus, there is a decrease in the expected improvement in activity with increased catalysts concentration, resulting in a plateau and decreasing linearity. A significant improvement in linearity was seen, however, at pH 10.8. This change in inhibition at pH 10.8, is likely the result of the easier release of carbonate, which is three times more abundant than bicarbonate at this higher pH. This was previously reported for a different CA mimic,[11] thus validating the results seen.

The differences between the effect of substrate concentration on the hydration or dehydration reactions suggests that the subsequent bicarbonate inhibition is more prevalent in the hydration reaction than the dehydration reaction. This is evident by the exponential slope for the hydration reaction compared to the linear slope for the dehydration reaction (Figure 1). This is the first time any inhibition for the dehydration reaction by a CA mimic has been observed.

Table 1 summarises the calculated k_{obs} values for both reactions across the pH and substrate concentration ranges studied. As mentioned previously, a decrease in k_{obs} is observed with increasing substrate concentration for both reactions. Additionally, the expected increase in hydration k_{obs} and expected increase in dehydration k_{obs}, with increasing and decreasing pH respectively, was seen. As generally observed in previous studies, [18, 33-34, 37] the hydration reaction was faster than dehydration at pH 8.2 and above, whereas the dehydration reaction was faster at pH 6.3. Interestingly, at pH 7.4, the two reactions had very similar observed rate constants at higher substrate concentrations. The hydration reaction was, however, slightly faster at the same substrate concentration. This is the first time that a CA mimic has been shown to have similar observed rate constants for both reactions at the same pH value. Furthermore, this is a change from the enzyme. CA only exhibits faster catalysis for the dehydration reaction over hydration at pH's below 7, [17, 22, 34, 36, 41] whereas the mimic ZnL1S demonstrates this at neutral pH.

In previous studies,[18, 22, 33-37] much larger HCO_3^- concentrations were used (of the order of x 10^{-3} M) and as the data here shows, this leads to catalyst inhibition. Therefore, previous studies concluded that hydration is much faster at pH 7.4. This study shows that under certain substrate conditions (i.e. at higher substrate concentrations), however, it is possible for ZnL1S to catalyse the dehydration reaction faster than the

hydration reaction at neutral pH values. This conclusion could likely be applied to other CA small molecule mimics as they share the same mechanism. The specific substrate concentrations required would vary depending upon the catalysts' affinity for bicarbonate.

Based upon its mechanism, it is expected that the relationship between hydration k_{cat} (the catalyst's rate constant independent of pH) and H^+ concentration should be linear. This is due to the activation of the catalyst with increasing pH as the zinc-bound water molecule is deprotonated (Scheme 1 Step 1).[33] Surprisingly, however, this relationship instead followed a power regression model (Figure S12A). The non-linearity of this trend suggests that there is a loss of inhibition with decreasing H^+ concentration (increasing pH). This leads to greater improvement of the k_{cat} values than expected from activation of the catalyst alone. At higher pH values, as well as the expected increase in hydration-active OH^--bound catalyst, there is an increased conversion to the weaker binding carbonate over bicarbonate, resulting in a faster release of product and thus decreasing inhibition.

In contrast, the catalyst's HCO_3^- dehydration activity increased linearly with increasing H^+ concentration (decreasing pH) (Figure S12B). This agrees with the catalyst's mechanism and previous investigations of other mimics, as more dehydration-active H_2O-bound catalyst was formed.[22, 35-36] We found that bicarbonate inhibition was not a significant limiting factor affecting the dehydration reaction. This contrasts with the hydration reaction, which was significantly impacted by the produced bicarbonate concentration, as seen by its non-linear slopes in Figures 1 and Figure S12.

The results thus far have shown that the catalysis of both the hydration and the dehydration reactions, by ZnL1S, are inhibited at higher concentrations of substrate. As pointed out previously (see introduction), the CO_2 hydration by ZnL1S and other mimics is rate-limited by the bicarbonate-bound state of the catalysts. [9-11, 17, 20, 27] The rate-limiting step of HCO_3^- dehydration is however currently unknown. Given the natural equilibrium between HCO_3^- and CO_2, it is also unclear which species is responsible for the observed inhibition of the dehydration reaction.

Capturing the Bicarbonate-bound Intermediate via NMR. To provide evidence for the dehydration reaction's rate-limiting step, an NMR study was undertaken to see if a bicarbonate-bound intermediate could be captured. Employing the Zn^{2+} complex in aqueous and non-aqueous solvents (D_2O and/or deuterated DMSO), both the hydration and dehydration reactions were studied. The study also allowed for a comparison of each reaction's NMR profile in each solvent.

There was no bound bicarbonate intermediate detected as part of the dehydration reaction in D_2O, due to the speed of the reaction relative to a typical NMR scan duration. It was apparent, however, that the reaction had proceeded to completion, as observed though a loss of HCO_3^- and production of CO_2 and H_2O (Figures S13 and S14). In DMSO, however, a bound Zn^{2+} bicarbonate intermediate (Figure 2), as well as the production of CO_2 and H_2O (Figures S15-17), could be observed as the mimic's turnover was slowed in this solvent. This suggests that the rate-limiting step of the dehydration reaction is also at the bicarbonate-bound intermediate stage, as is the case with the hydration reaction.

Evidence of the hydration reaction was not detected in DMSO (Figures S18 and S19), due to the inability of the bound water molecule to deprotonate as per the first step of the catalyst's mechanism (Scheme 1), and as seen for a different CA mimic.[42] In D_2O, however, production of free HCO_3^- by the hydration reaction was observed, although the intermediate of the hydration reaction was not detected. The latter is not surprising, given the fast reaction times for the hydration reaction as compared to the speed at which a NMR scan reaches completion (Figures S20 and S21).

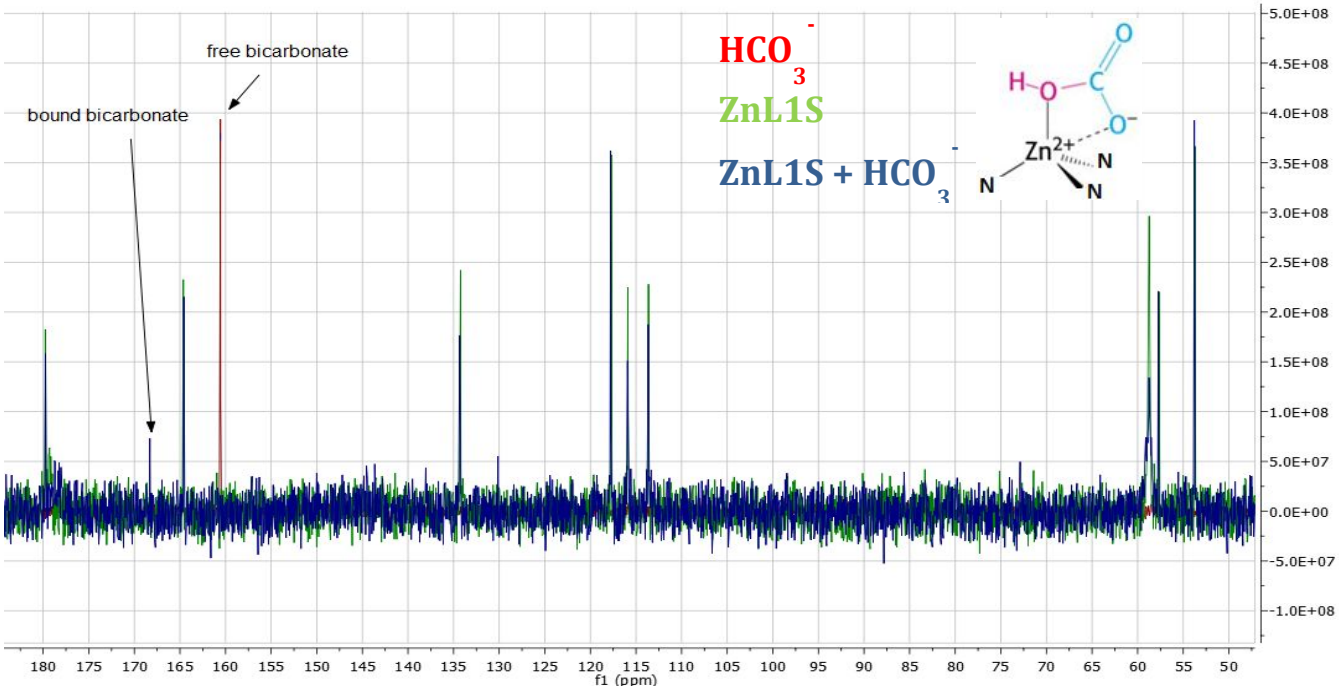

Figure 2. ^{13}C NMR spectrum in DMSO comparing free bicarbonate, ZnL1S and ZnL1S with bicarbonate illustrating the ability of ZnL1S to bind to bicarbonate. Free bicarbonate is seen at 160 ppm and bound bicarbonate at 167 ppm. ZnL1S peaks at 180, 165, 135, 117, 116, 114, 59 and 54 ppm. Peak at 57 ppm is due to ethanol used to enhance the solubility of sodium bicarbonate with the complex in d-DMSO.

To visualise the bicarbonate-bound intermediate through NMR during the hydration reaction, attempts were made to slow down the reaction through the addition of the hydration product HCO_3^-. By adding HCO_3^- into the hydration reaction as catalysed by ZnL1S, the activity of the catalyst should slow down as the equilibrium is pushed back towards the substrate CO_2. This effect on the hydration rate by addition of HCO_3^- has been seen previously with a different CA mimic, although not via NMR but through the observed effect on the mimic's kinetics via stopped-flow.[11] Furthermore, the addition of a product mimic, such as NO_3^-, should inhibit ZnL1S sufficiently to allow the bicarbonate-bound intermediate to be captured. With increasing concentrations of HCO_3, evidence of increased zinc-bound bicarbonate was seen with an increasing upfield shift of the aromatic ^1H NMR peaks of the complex ligand (Figure S22). Additionally, upon introduction of NO_3^-, a slight upfield shift was again seen indicating zinc-bound bicarbonate or nitrate, although it is unknown which one is bound. Regardless, this demonstrates that when the hydration reaction is slowed, the intermediate rate-limiting bicarbonate-release step can be captured.

In summary, it was shown that the catalyst behaves as expected by undergoing both reactions under the appropriate conditions. Most importantly however, evidence of the intermediates of both reactions were captured demonstrating the complex's ability to strongly bind bicarbonate.

Effect of CO_2 Hydration Substrate and Product Mimics on ZnL1S CO_2 Hydration Activity. To further confirm the likely inhibitory species, (CO_2 or HCO_3^-), the inhibitory effect of CO_2 and HCO_3^- mimics on ZnL1S hydration activity was undertaken. It is well established that CA enzymes can be inhibited by a range of anions such as Cl^-, Br^-, NCS^-. These anions bind via replacement of the coordinated water molecule or via direct insertion into the active site, thus increasing the coordination number around the zinc centre.[21-24] They have previously been tested on other CA mimics, such as the well-studied mimic zinc cyclen as well as ZnL1S. [9-10, 17, 24]

In this study, a wider range of potential inhibitors were chosen, including those previously studied. Potential inhibitors were selected that are structurally and electronically related to either CO_2 or HCO_3^-, the reactants for the CA catalysed reactions. The commercially available CA inhibitor acetazolamide was also tested to compare its binding to the enzyme and its synthetic mimic. Charge, geometry and localisation of electrons were all key factors in choosing the inhibitors employed (Table S4 for details). As can been seen from the data presented in Figure 3, neutral species such as the linear CS_2 or bulky DIC (both resembling CO_2) and trigonal planar urea were not inhibitory. Charged tetrahedral species showed a mixed response. Phosphate was the only tetrahedral species revealing significant inhibition, whereas sulfate and perchlorate did not inhibit the ZnL1S catalysed CO_2 hydration. Single-charge inhibitors with planar geometry (e.g. chloride, thiocyanate, nitrite, bicarbonate, formate and nitrate) were all inhibitory, although nitrate and thiocyanate were the most potent. Interestingly, the well-known sulfonamide CA enzyme inhibitor acetazolamide was the most effective inhibitor of the tested compounds.

The inhibitory constants for the most potent ionic inhibitors, nitrate and thiocyanate, were therefore determined. The IC_{50} for NO_3^- of 4.236 x 10^{-5} M is about two times smaller than that observed for SCN^- 8.791 x 10^{-5} M. A two-sample t-test (16) = 27.34, p= <0.0001 shows that there is a statistically significant difference between the two IC_{50} values. Both NO_3^- and SCN^- share a single negatively charged planar geometry, which may reflect the transition state of the Zn-bicarbonate complex (see Scheme 1 between step 3 and 4). In particular, NO_3^- shares charge and geometry with HCO_3^-, and hence has been used previously to explore bicarbonate binding to CA mimics.[43] SCN^- shares only its linear shape with CO_2 and thus, may well comprise the charge of the HCO_3^- with the shape of the CO_2, making it a transition state mimic. Since the inhibitory potency correlates with its affinity for the catalyst, one can conclude that bicarbonate mimicking inhibitors (e.g. nitrate) are better in binding to the catalyst than the carbon dioxide mimicking test compounds (e.g. CS_2; DIC). This in turn indicates a preference of the ZnL1S catalyst for binding bicarbonate over CO_2. This inhibitor profiling, demonstrates that bicarbonate mimics are stronger inhibitors of, and thus bind more strongly to, ZnL1S than CO_2 mimics. This corroborates the data presented so far and provides further evidence that the bicarbonate-bound intermediate is the most likely rate-limiting step. This is in agreement with similar smaller investigations for other CA mimics.[9-11, 17, 20, 27] The IC_{50} and k_i values for the CA enzyme inhibitor acetazolamide were determined for the inhibition of the CO_2 hydration reaction (6.99 x 10^{-6} M and 3.14 x 10^{-6} M respectively). This is evidence that the Zn-complex, without the surrounding amino acids in the enzyme's active site, is sufficient for the interaction of this important drug molecule within the catalytic cavity of CA enzymes.[24, 44-46]

The effect of pH (9.5 versus 10.8) was examined via the inhibition of ZnL1S by the tested compounds to see how it affects the inhibitor profile. Specifically, the effect that the ratio of bicarbonate to carbonate has either side of their pKa of 10.3 was observed. Only $NaHCO_3$ showed a significant effect, with a stronger inhibitory potency at pH 9.5 than at pH 10.8.The increased concentration of the weaker binding carbonate, over the stronger binding bicarbonate, at higher pH was the reason for this difference, as discussed earlier.

The effect of inhibitors on the dehydration reaction (Figure S23) yields similar results to that of the hydration reaction. It was observed that those compounds that most similarly mimic bicarbonate (i.e. charged species) inhibit ZnL1S dehydration most significantly at pH 6.3. Interestingly, the addition of CO_2 resulted in a decrease in activity of 27%. This can be attributed to the push back of the equilibrium by introducing the product into the reaction mixture, resulting in slower dehydration activity. Overall, the dehydration reaction seems to be more susceptible to inhibition by these mimics than the hydration reaction, although the sequence of inhibitor strength and compound is the same for both reactions.

Following this, study of the effect of CO_2 and HCO_3^- mimics on the typical CA reactions and the effect of CO_2 and HCO_3^- on non-CA catalysis by ZnL1S was explored for further evidence of the rate-limiting species.

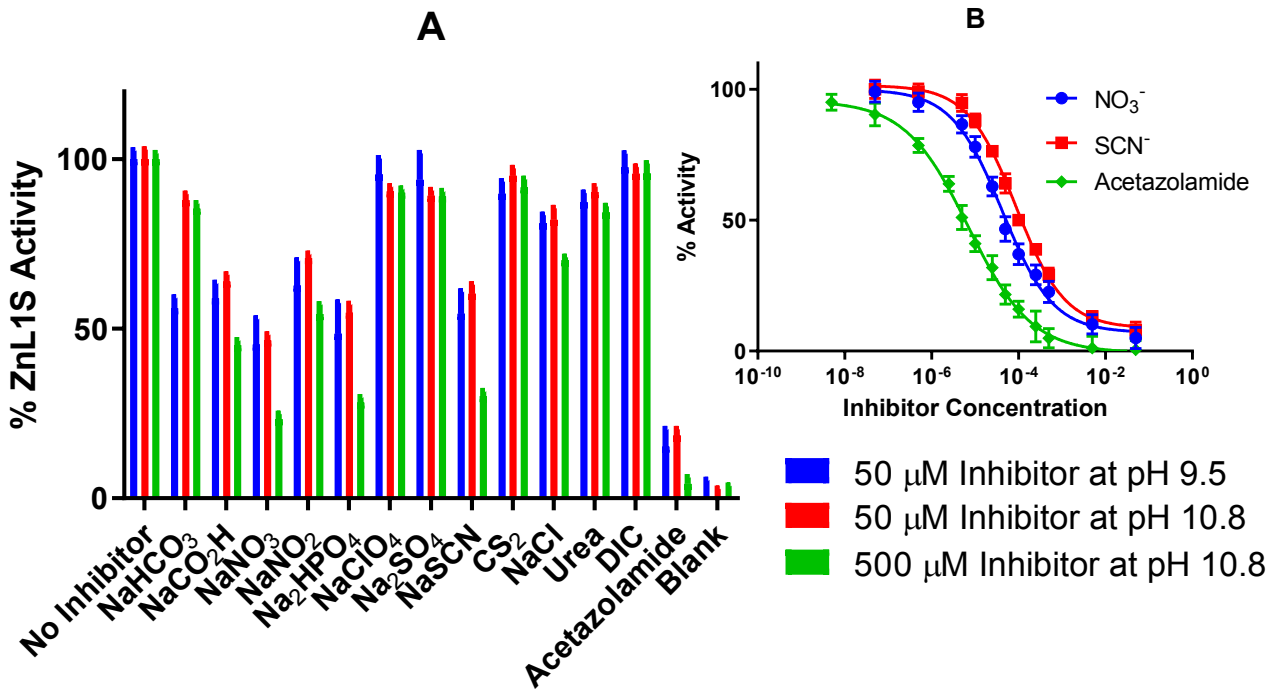

Figure 3. (A) The effect of different substrate mimics and known CA inhibitors on the % activity of CO_2 hydration by 50 μM ZnL1S over a range of pH and inhibitor concentrations. **(B)** The IC_{50} curves for the inhibitors NO_3^-, SCN^- and acetazolamide on the activity of CO_2 (1.69 mM) Hydration by 5 μM ZnL1S at pH 10.8. All data is the average of three repeats of three. Error bars are the standard deviation (N = 9).

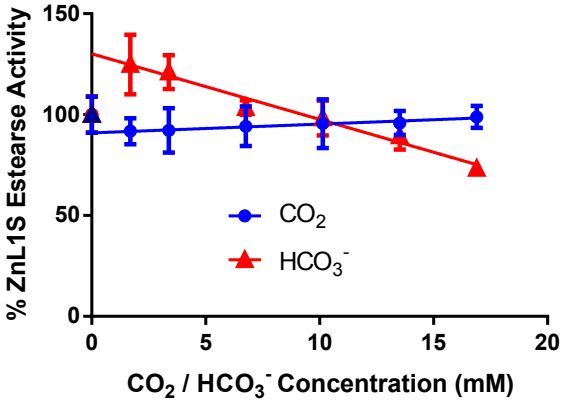

Figure 4. Effect of addition of CO_2 and HCO_3^- on the hydrolysis of 4-nitrophenyl acetate by 500 μM ZnL1S. Reactions were monitored at 348 nm. Data is the average of three repeats of three. Error bars represent the standard deviation (N = 9). The linear fit excludes 0 mM CO_2 / HCO_3^-.

The effect of CO_2 and HCO_3^- on ZnL1S Esterase Activity. It has been well documented that CA synthetic mimics demonstrate esterase activity by catalysing the hydrolysis of esters, typically 4-nitrophenyl acetate, into their respective alcohols and carboxylic acids (or their respective conjugate bases), although at much lower rates than their CO_2 hydration and HCO_3^- dehydration activities.[23, 46-48] The effect of increasing concentrations of either CO_2 or HCO_3^- on the esterase activity of ZnL1S (Figure 4) (measured by the conversion of 4-nitrophenyl acetate into 4-nitrophenolate and acetate) provides an alternative method of finding evidence for the rate-limiting step. CO_2 showed no significant inhibition, whereas HCO_3^- inhibited the esterase activity with increasing concentrations from 1.69 mM to 16.9 mM HCO_3^-. There was an initial activity rise from the associated increase in pH from bicarbonate. The results demonstrate that HCO_3^- binds to the zinc centre causing an inhibition of the esterase activity of the catalyst. In contrast, no binding was observed for CO_2, thus this data supports the conclusion drawn from the NMR experiments described above, and provides evidence for previous predictions made by other investigations for both ZnL1S and other CA mimics.[9-11, 17, 20, 27] Interestingly, this is the first time bicarbonate inhibition of esterase activity has been shown for ZnL1S, which complements similar data obtained with a different CA mimic.[46]

Effect of Metal Centre. The experimental evidence in this study has shown that the rate-limiting step for both the hydration and dehydration reactions by ZnL1S is at the bicarbonate-bound intermediate step. To better understand the reasons behind the mechanism, and thus to see if the preference for either reaction can be changed, we investigated the role of the metal centre on the rate of hydration and dehydration of ZnL1S. To achieve this, the

L1S ligand was complexed to several different transition metals, Cu, Ni and Co, instead of Zn (Scheme S3). While previous investigations with other mimics confirmed zinc's superiority for catalytic behaviour,[16-19] the L1S ligand chelation to different metal centres had yet to be explored. Furthermore, the effect of metal centre on dehydration activity has not been investigated before for any CA mimic. The three novel transition metal complexes of L1S were successfully synthesised (Supporting Information section 1c), which were subsequently tested for their ability to catalyse both the hydration reaction and dehydration reactions.

The experimentally observed rate constants for CO_2 hydration were measured for each transition metal complex at pH 9.5, 8.2, and 7.4 using a typical CO_2 hydration measurement (Figure S24 and Table 2 for results). As expected from the mechanism, the catalysts were most active for CO_2 hydration at pH 9.5. There was, however, a non-linear trend between proton concentration and k_{cat}, demonstrating that all the catalysts suffered from bicarbonate inhibition regardless of metal centre. The order of activity for the transition metal L1S complexes at pH 9.5 was ZnL1S > CoL1S > CuL1S > NiL1S.

Table 2. Summary of k_{obs} for the hydration of CO_2 and dehydration of HCO_3^- by CA mimics at multiple pH's.

	Metal Centre	Zn	Cu	Ni	Co
CO_2 Hydration k_{obs} ($M^{-1}s^{-1}$)	pH 9.5	8803 ± 550.3	4478 ± 523.6	3489 ± 347.7	5766 ± 670.6
	pH 8.2	574.5 ± 34.59	93.6 ± 20.70	35.1 ± 15.77	102.4 ± 19.98
	pH 7.4	128.3 ± 14.43	44.3 ± 12.55	Below LOD	Below LOD
HCO_3^- Dehydration k_{obs} ($M^{-1}s^{-1}$)	pH 6.3	102.1 ± 12.98	44.3 ± 9.91	Below LOD	79.6 ± 10.08
	pH 7.4	8.5 ± 0.57	3.01 ± 0.49	Below LOD	5.9 ± 0.63
	pH 8.2	5.1 ± 0.52	Below LOD	Below LOD	Below LOD

The data is the average of three repeats. k_{obs} data calculated from the fit of the data in Figure S24 and S25. LOD= limit of detection.

As predicted, ZnL1S was shown to be the fastest catalyst for CO_2 hydration, in alignment with other CA mimic studies investigating the effect of alternative metal centres. [16-19] The higher observed rate constant for CoL1S over CuL1S and NiL1S, was attributed to the similar coordination chemistry of Zn(II) and Co(II), and the fast interconversion of these two metals between four-, five- and six-coordination states,[49] as well as the similar ionic radii (88 for Zn(II) cf. 88.5 for Co(II)).[50] This trend of ZnL1S > CoL1S > CuL1S > NiL1S directly correlates with the likelihood of the metal centres to form bidentate coordination to bicarbonate, Ni > Cu > Co > Zn. As described by Han *et al.*,[43] Zn(II) derivatives bind to bicarbonate with unidentate coordination, and the Co(II) derivatives show binding that was intermediate between unidentate and bidentate. In contrast, the Cu(II) and Ni(II) derivatives show a higher tendency to exhibit bidentate coordination.[43] Furthermore, the similar pKa values (8.28 for Co and Ni and 8.29 for Cu and Zn) exclude the pKa of the metal-bound water as a determining factor for the differences seen in the interconversion of CO_2/HCO_3^- between the metal complexes. The tighter binding of bicarbonate results in the slower release of product, resulting in slower rates of hydration. This is especially true at lower pH's as illustrated by the non-linear pH dependency. Thus, the importance of overcoming the rate-liming step by reducing bicarbonate affinity for the metal centre is emphasised.

The initial activity for HCO_3^- dehydration was measured for each transition metal complex at pH 6.3, 7.4 and 8.2 (Figure S25 and Table 2 for results). As expected from the mechanism, the catalysts were most active for HCO_3^- dehydration at pH 6.3. The linear trend between proton concentration and k_{cat} for all active catalysts, demonstrated minimal bicarbonate inhibition for these mimics. It can be observed from the data that ZnL1S is the superior catalyst for HCO_3^- dehydration at pH 6.3 and pH 7.4, followed closely by CoL1S. A similar trend in rate constant was observed at pH 6.3 and pH 7.4, as seen for the hydration reaction at pH 9.5. This also correlated with strength of bicarbonate binding. Tighter binding would result in a slower catalytic rate, for both CO_2 hydration and HCO_3^- dehydration, and could explain why no activity was observed for NiL1S.

This study showed that the zinc metal centre generated the fastest rates and k_{obs} for both the hydration and dehydration reactions, followed by cobalt, copper and then nickel. The zinc centre was therefore key to the ability of the catalyst to efficiently hydrate CO_2 and dehydrate HCO_3^- due to its preferred weaker monodentate binding to bicarbonate. This demonstrates just how important bicarbonate affinity is in determining the mimic's activities and overcoming the rate-limiting step.

Future Improvements in Catalyst Activity through Strategic Ligand Design. As discussed, it is desired that rates as fast as that of the natural CA enzyme can be achieved by its synthetic mimics. For this goal to be reached, the effect of bicarbonate inhibition needs to be addressed. The zinc centre within CA mimics is highly electron deficient and therefore easily coordinates to anions, such as bicarbonate. Although it is not the case for ZnL1S, this effect is often enhanced further in many reported CA mimic complexes, due to their cationic nature, which attract anionic species into their secondary coordination sphere to maintain charge balance, which drives the equilibrium to the bicarbonate-bound species.[10]

Our work has shown that the limitations of bicarbonate binding, resulting in slower activity, should be addressed in the development of future CA mimics. There are two potential ways in which this could be achieved; (i) reducing the affinity of the anion for the zinc centre to discourage strong bicarbonate binding and (ii) facilitating the approach of water into the hydrophobic pocket around the zinc atom to displace the bicarbonate anion. Both can be primarily achieved through intelligent ligand design.

To reduce anion affinity for the metal centre, more electron donating ligands should be used. The ligand L1S, employed in this study, is a good example of this, as it is an anionic, water-soluble, salen-like ligand, that has the ability to donate electron density into the metal centre and therefore facilitates dissociation of bicarbonate and thus improves the rate of CO_2 hydration.[9-10] This is part of the reason why ZnL1S is the fastest small molecule CA mimic seen in the literature.

The other reason why ZnL1S is highly active for CO_2 hydration is that Nakata *et al.* designed the mimic to contain a hydrophobic pocket which facilitates the approach of CO_2 for hydration.[24] The approach of water to displace the formed bicarbonate is however, consequently unfavourable, thus rate-limiting the catalyst. To overcome this, a ligand should include the ability to be able to induce an extensive hydrogen bonding network in the proximity of the metal centre, much like the natural enzyme CA, which achieves this by utilising three hydrogen bonding amino acids.[28-30] For this reason, carbonic anhydrase is limited not by bicarbonate release but by the shuttle of protons,[26] and therefore is significantly faster than any synthetic mimic reported to date.[27] With the structural changes recommended, even greater improvements in catalytic activities could be achieved.

Comparison of ZnL1S Kinetic Properties to CA and other CA mimics. Historically, CA mimics have struggled to match the hydration activity of the natural enzyme (e.g. hCA II hydration k_{cat} / k_m of 1.5 x 10^8 M^{-1} s^1).[51] Using a lower concentration of substrate (1.69 mM CO_2), we have however, achieved a step in the right direction towards this goal. The hydration k_{cat} achieved by ZnL1S in this study is the highest reported by a small-molecule CA mimic catalyst to date. With a k_{cat} of 28,093 M^{-1} s^{-1}, ZnL1S has a catalytic rate that is over five times faster than that of the next best small molecule mimic, Zn Cyclam, with a k_{cat} of 5040 M^{-1} s^{-1} (Table S5). By employing a lower concentration of substrate, ZnL1S was found to be almost three times faster than had been previously predicted from the low temperature study reported by Nakata *et al.*[24] and thus, a better idea of the true potential of the catalyst for CO_2 hydration was seen. Furthermore, it is possible that decreasing the CO_2 concentration further, could improve the k_{cat} beyond the value reported here, but this concentration falls below our current methodology's limit of detection. At pH 10.8, the k_{cat} of ZnL1S is similar to that of the recent synthetic metalloenzyme developed by Zastrow *et al.*[52], which at the time demonstrated the highest recorded rate of CO_2 hydration for a CA mimic.[52] At pH 9.5 however, the metalloenzyme was faster. This metalloenzyme is, however, significantly larger and protein-like, and therefore suffers from a lower thermal stability and more complex synthesis than a small-molecule mimic like ZnL1S.

CA mimics have also struggled to match the dehydration activity of the natural enzyme (e.g. hCA II dehydration k_{cat} / k_m of 1.2 x 10^7 M^{-1} s^{-1}).[53] The dehydration k_{cat} for ZnL1S described here has shown a 60% improvement of that previously reported for the mimic, as measured via the weight-loss method.[37] ZnL1S has a dehydration k_{cat} of 579 M^{-1} s^{-1} which is over ten times that of the next fastest mimic Zn Cyclen, with a k_{cat} of 55 M^{-1} s^{-1} (Table S5). ZnL1S has therefore shown the fastest dehydration k_{cat} reported for a small molecule CA mimic to date. Consequently, this work represents a significant step towards matching the activity demonstrated by CA. Comparing the k_{cat} values for the hydration and dehydration reactions, ZnL1S shows preference for the hydration reaction rather than dehydration, as is the case for both the enzyme and other CA mimics published previously.

Simply by reducing the concentration of substrate used for both the hydration and dehydration reactions, we have reported increases in catalytic rates due to weaker bicarbonate binding. This has been without the need for any modifications to the complex's structure. It is expected that this principle could be applied to any CA mimic used for CO_2 capture, that follows the same mechanism as ZnL1S and therefore has the same rate-limiting step.

Comparison of Inhibitor Effects on ZnL1S and CA. In the previously discussed inhibitor study, it was observed that the negatively charged species were more inhibitory for the mimic (μM range K_i) than for the enzyme (mM range K_i) (Table 3). It is likely that it is easier for the anions to enter the active site of the complex and compete with substrates in the more solvent exposed centre. The opposite was true for acetazolamide where it was more inhibitory for the enzyme (nM range K_i) over the mimic (μM range K_i) (Table 3). This is probably caused by lack of acetazolamide binding amino acids for the mimic, as well as an increased steric hindrance when acetazolamide binds to ZnL1S.[24] The application of inhibitor profiling (which is commonly used to characterise enzymes) to probe the hydration mechanism of CA mimics revealed new insights into how binders interact differently between native CA and its mimics.

Table 3. Comparison of inhibition data for the complex ZnL1S with data from different isoforms of human CA (hCA).

	IC_{50}	K_i			
	ZnL1S		hCA I	hCA II	hCA VI
Acetazolamide	6.99 ± 0.50 μM	3.14 μM	250 nM	12 nM	11 nM

NO_3^-	42.36 ± 2.93 µM	27.9 µM	7 mM	35 mM	0.76 mM
SCN^-	87.91 ± 4.05 µM	59.8 µM	0.2 mM	1.6 mM	0.89 mM

ZnL1S CO_2 hydration data was measured using 5 µM ZnL1S and 1.69 mM CO_2 at pH 10.8 and 25°C. Data is the average of three repeats. Enzyme data is from Bertucci *et. al.* and Supuran *et. al.*, measured using 235 nM hCA I and 1.5 nM hCA II and VI, at pH 7.5 and 20°C.[54-55]

ZnL1S only showed inhibition by bicarbonate and no inhibition by carbonate. Whereas it has been shown that hCA II is inhibited by both bicarbonate and carbonate, although the inhibition is significantly weaker for the enzyme (K_i = 85 and 73 mM for bicarbonate and carbonate respectively) [56] than for ZnL1S (nearly 50% reduction in activity with 50 µM HCO_3^-). It should be noted that there is no observable difference between inhibition of CA by bicarbonate or carbonate, as bicarbonate release is not the rate-limiting step for the natural enzyme, highlighting further the different rate limiting steps between the native enzyme and its mimics. It is also worth noting that our data reveal a much less potent effect of chloride on ZnL1S activity than previously reported, [24] which could be due to the ZnL1S complex being generated *in situ* in the stopped-flow by Nakata *et. al.*, potentially resulting in inhibition of the initial formation of the catalyst.

Comparison of Small-Molecule Mimic and Enzyme Kinetic Analysis Methodologies. Interestingly, there is a difference observed in the literature between the analysis methods employed to study rates of catalysis by enzymes with that used for their mimics. For more information on the different analysis methodologies see Supporting Information Section 2g. In brief, the kinetic data for ZnL1S was analysed via the typical enzyme analysis methodology generating "*enzyme-like*" kinetic parameters. The result of this is described below and in Figure S26 and Table S6. To avoid confusion, the kinetic parameters generated by the enzyme and catalysis analysis methods will be labelled with a superscript e (for enzyme) or c (for catalyst) respectively.

Typically, the k_{cat}/k_m^e of enzymes are compared to the k_{cat}^c of synthetic mimics, as they have the same units (M^{-1} s^{-1}) and both quantify catalytic efficiency. Upon comparison of the k_{cat}/ k_m^e of ZnL1S to the k_{cat}^c of ZnL1S, a difference in the values can be seen. For both reactions and across all conditions studied, the calculated k_{cat}/ k_m^e values were greater than their respective mimic-like k_{cat}^c, often by orders of magnitude. As the k_{cat}/ k_m^e considers the effect of substrate concentration and the subsequent inhibition, it can be said that these values demonstrate a better representation of the mimic's ability to catalyse each reaction. These values show the mimic's maximal catalytic efficiency when substrate concentration is negligible (at a particular concentration of catalyst). This is rather than the catalytic efficiency per molar of catalyst at a specific substrate concentration, as often reported.

Consequently, a comparison of the k_{cat}/ k_m^e of ZnL1S to that of hCA II allows for a better indication of the closeness/ difference between the activities of each species. The hydration catalytic efficiency (k_{cat} / k_m^e) of hCA II at pH 9.0 is 1.5 x 10^8 M^{-1} s^{-1}, whereas the highest catalytic efficiency (k_{cat} / k_m^e) of ZnL1S, at a similar pH, in this study was found to be 5.9 x 10^5 at pH 9.5. At pH 10.8, an even greater catalytic efficiency was found (2.0 x 10^7 M^{-1} s^{-1}). The maximum efficiency of ZnL1S hydration, i.e. with no inhibition, is therefore only 2.5 magnitudes smaller than that of hCA II at similar pH. This is a significant improvement when compared to the k_{cat}^c calculated previously using the small-molecule methodology, which gave a value of 2.8 x 10^4 M^{-1} s^{-1} at pH 9.5 using 1.69 mM CO_2.

The previously discussed metalloenzyme mimic developed by Zastrow *et al.*, which had a catalytic efficiency (k_{cat} / k_m^e) of 1.8 x 10^5 M^{-1} s^{-1} at pH 9.5.[52] ZnL1S is now over three times more efficient at the same pH. When not inhibited by bicarbonate, ZnL1S therefore has the potential to be the fastest mimic of CA ever synthesised. Furthermore, the k_{cat}/ k_m^e of ZnL1S increased with decreasing concentration of mimic and therefore the maximal catalytic efficiency could be even greater than reported here. A lower concentration of mimic could not be measured in this study due to the limit of detection of our current experimental methodology. Nevertheless, it is entirely feasible that with a lower concentration of mimic, catalytic efficiencies closer to that of CA could be achieved.

The same conclusions can be drawn for the dehydration reaction. The dehydration catalytic efficiency (k_{cat} / k_m^e) of hCA II is 1.2 x 10^7 M^{-1} s^{-1} at pH 5.5,[53] whereas the highest catalytic efficiency (k_{cat} / k_m^e) of ZnL1S in this study was found to be 1.7 x 10^4 M^{-1} s^{-1} at pH 6.3. The maximum efficiency of ZnL1S dehydration, i.e. with no inhibition, is therefore only 3 orders of magnitude smaller than that of hCA II. This is significantly higher when compared to the value of k_{cat}^c calculated previously, 579 M^{-1} s^{-1} at pH 6.3 using 1.5 mM HCO_3^-. Our work has revealed that ZnL1S is the fastest small-molecule water-soluble CA mimic for dehydration reported to date. As with the case for the hydration reaction, ZnL1S has the potential to be an even greater catalyst for HCO_3^- dehydration with a lower concentration of mimic and potentially reach catalytic efficiencies similar to that of CA.

Conclusions. We report for the first time the rate-limiting step of the dehydration reaction by a CA mimic to be at the bicarbonate-bound step, much like the hydration reaction. This confirms that it is the mimic's affinity for bicarbonate that results in the previously observed hydration inhibition, and not the occurrence of the reverse dehydration reaction. Each reaction is however inhibited by bicarbonate by differing degrees, with the hydration reaction demonstrating significantly greater bicarbonate inhibition than the dehydration reaction. With this knowledge, the catalyst's preference for either reaction could be controlled via substrate concentration.

Consequently, a significant increase in the activity of the previously published CA mimic ZnL1S, which is the fastest small-molecule mimic published to date, was achieved without the need for modification of the catalyst

structure. Rather, by simply lowering the concentration of the substrate used for either the hydration of CO_2 or dehydration of HCO_3^-, we were able to achieve an increase in k_{cat} by a factor of 3 and 1.6 respectively. By lowering the concentration of substrate, especially for the hydration reaction, the energetically unfavourable rate-limiting bicarbonate-intermediate step was overcome due to the subsequently lower concentration of bicarbonate. This information will be critical for optimising the use of such mimics in industrial carbon capture.

Conversely, by increasing the substrate concentration used, similar k_{obs} could be seen for both reactions at the same pH (pH 7.4) for the first time. This opens the potential to manipulate mimics to enable them to show preference to catalyse HCO_3^- dehydration over CO_2 hydration at physiological pH values. As demonstrated by the maximal catalytic efficiencies (k_{cat} / k_m^e) of ZnL1S at negligible substrate concentration, the mimic could reach activities of only 2.5-3 orders of magnitude slower than that of the natural CA enzyme itself. This finding could likely be applied to any CA, and thus these mimics have the potential to demonstrate significantly higher catalytic activities in the future. With future careful ligand design, to facilitate bicarbonate release at a faster rate, even greater activities could also be reached.

Additionally, within this study, the observed rate constants (k_{obs}^c) for CO_2 hydration and HCO_3^- dehydration catalysed by ZnL1S, CuL1S, NiL1S and CoL1S, (except ZnL1S for CO_2 hydration), were reported for the first time via stopped-flow. A comparison of the kinetic activity of this suite of CA mimics with differing metal centres revealed that ZnL1S was a superior catalyst for both the CO_2 hydration and HCO_3^- dehydration reactions as expected. The kinetic profile of ZnL1S for both hydration and dehydration activities was studied across a large pH, complex and substrate concentration range at 25°C. Consequently, substrate inhibition kinetics, caused by increased bicarbonate, were seen for the first time for a CA mimic. A comparison between analytical methodologies of catalysts and enzymes was carried out, and the same trends could be seen, and subsequent conclusions drawn.

Finally, this work contains the largest inhibitor study of any CA mimic reported in the literature. The first IC_{50} and K_i values for the hydration of CO_2 by CA mimic inhibitors are also reported, for both anionic inhibitors and the commercial CA inhibitor acetazolamide. The use of substrate and product mimics to probe the mechanism of enzyme mimics, as shown here for CA and its small molecule mimic ZnL1S, allows for a subsequent deeper understanding revealing differences between the substrate binding in the enzyme and its mimics, as well as the difference in mechanisms that this alludes to. In the case of the natural CA enzyme and the ZnL1S mimic, small anions were found to be more inhibiting for the mimic, suggesting a greater importance for anion binding affinity in the mechanism of CA mimics than the enzyme. This approach could be used to investigate any other chemical mimic of a biological enzyme, especially those that are important in medicine, such as is the case with the CA studied here.

Future work will look at how these findings, especially the effect of substrate concentration to manipulate preference for either reaction at physiological pH and the potential to improve catalytic activity further, can be applied to uses of CA and its mimics for wider-world applications.

ASSOCIATED CONTENT

All ligand and complex spectra, as well as data from the stopped-flow and all other assays can be found in the attached Supporting Information. This material is available free of charge via the Internet at http://pubs.acs.org

ACKNOWLEDGEMENT

Thank you to Dan Scott and Andy Ashley at Imperial College London for their assistance with the Topeler pump for the ^{13}C CO_2 NMR studies. Thank you to Lisa Haigh for operation of the Imperial College London Chemistry Mass Spectrometry service. Thank you to Stephen Boyer at the Elemental Analysis Service at London Metropolitan University. This work was supported by an EPSRC Centre for Doctoral Training Studentship from the Institute of Chemical Biology (Imperial College London) awarded to Jonathan Rains.

REFERENCES

1. Bouzalakos, S.; Mercedes, M. Overview of Carbon Dioxide Capture and Storage Technology. In *Developments and Innovation in Carbon Dioxide (CO_2) Capture and Storage Technology*, 1 ed.; Maroto-Valer, M. M., Ed. Woodhead Publishing Ltd.: University of Nottingham, UK, 2010; Vol. 2.

2. Ma, J.; Sun, N.; Zhang, X.; Zhao, N.; Xiao, F.; Wei, W.; Sun, Y., A Short Review of Catalysis for CO_2 Conversion; *Catalysis Today* **2009,** *148*, 221-231.

3. Ranjan, M.; Herzog, H. J., Feasibility of Air Capture; *Energy Procedia* **2011,** *4*, 2869-2876.

4. Lindskog, S., Structure and Mechanism of Carbonic Anhydrase; *Pharmacol. Ther.* **1997,** *74*, 1-20.

5. Domsic, J. F.; Avvaru, B. S.; Kim, C. U.; Gruner, S. M.; Agbandje-McKenna, M.; Silverman, D. N.; McKenna, R., Entrapment of Carbon Dioxide in the Active Site of Carbonic Anhydrase Ii; *J. Biol. Chem.* **2008,** *283*, 30766-30771.

6. Supuran, C. T., Structure and Function of Carbonic Anhydrases; *Biochem. J.* **2016,** *473*, 2023-2032.

7. Nath, I.; Chakraborty, J.; Verpoort, F., Metal Organic Frameworks Mimicking Natural Enzymes: A Structural and Functional Analogy; *Chem. Soc. Rev.* **2016,** *45*, 4127-4170.

8. Saeed, M.; Deng, L., CO_2 Facilitated Transport Membrane Promoted by Mimic Enzyme; *J. Membr. Sci.* **2015,** *494*, 196-204.

9. Kelsey, R. A.; Miller, D. A.; Parkin, S. R.; Liu, K.; Remias, J. E.; Yang, Y.; Lightstone, F. C.; Liu, K.; Lippert, C. A.; Odom, S. A., Carbonic Anhydrase Mimics for Enhanced CO_2 Absorption in an Amine-Based Capture Solvent; *Dalton Trans.* **2015,** *45*, 324-333.

10. Lippert, C. A.; Liu, K.; Sarma, M.; Parkin, S. R.; Remias, J. E.; Brandewie, C. M.; Odom, S. A.; Liu, K., Improving Carbon Capture from Power Plant Emissions with Zinc- and Cobalt-Based Catalysts; *Catal. Sci. Technol.* **2014,** *4*, 3620-3625.

11. Floyd, W. C., 3rd; Baker, S. E.; Valdez, C. A.; Stolaroff, J. K.; Bearinger, J. P.; Satcher, J. H., Jr.; Aines, R. D., Evaluation of a Carbonic Anhydrase Mimic for Industrial Carbon Capture; *Environ. Sci. Technol.* **2013,** *47*, 10049-10055.

12. Wong, S. E.; Lau, E. Y.; Kulik, H. J.; Satcher, J. H.; Valdez, C.; Worsely, M.; Lightstone, F. C.; Aines, R., Designing Small-Molecule Catalysts for CO_2 Capture; *Energy Procedia* **2011,** *4*, 817-823.

13. Ibrahim, M. M.; Shaban, S. Y.; Ichikawa, K., A Promising Structural Zinc Enzyme Model for CO_2 Fixation and Calcification; *Tetrahedron Lett.* **2008,** *49*, 7303-7306.

14. Ibrahim, M. M.; Amin, M. A.; Ichikawa, K., Synthesis and Characterization of Benzimidazole-Based Zinc Complexes as Structural Carbonic Anhydrase Models and Their Applications Towards Co2 Hydration; *J. Mol. Struct.* **2011,** *985*, 191-201.

15. Jin, C.; Zhang, S.; Zhang, Z.; Chen, Y., Mimic Carbonic Anhydrase Using Metal-Organic Frameworks for CO_2 Capture and Conversion; *Inorg. Chem.* **2018,** *57*, 2169-2174.

16. Bergquist, C.; Fillebeen, T.; Morlok, M. M.; Parkin, G., Protonation and Reactivity Towards Carbon Dioxide of the Mononuclear Tetrahedral Zinc and Cobalt Hydroxide Complexes, [Tp(Bu)T(,Me)]Znoh and [Tp(Bu)T(,Me)]Cooh: Comparison of the Reactivity of the Metal Hydroxide Function in Synthetic Analogues of Carbonic Anhydrase; *J. Am. Chem. Soc.* **2003,** *125*, 6189-6199.

17. Lau, E. Y.; Wong, S. E.; Baker, S. E.; Bearinger, J. P.; Koziol, L.; Valdez, C. A.; Satcher, J. H., Jr.; Aines, R. D.; Lightstone, F. C., Comparison and Analysis of Zinc and Cobalt-Based Systems as Catalytic Entities for the Hydration of Carbon Dioxide; *PloS one* **2013,** *8*, e66187.

18. Davy, R.; Shanks, R. A.; Periasamy, S.; Gustafason, M. P.; Zambergs, B. M., Development of High Stability Catalysts to Facilitate CO_2 Capture into Water–an Alternative to Monoethanolamine and Amine Solvents; *Energy Procedia* **2011,** *4*, 1691-1698.

19. Keum, C.; Kim, M.-C.; Lee, S.-Y., Effects of Transition Metal Ions on the Catalytic Activity of Carbonic Anhydrase Mimics; *J. Mol. Catal. A: Chem.* **2015,** *408*, 69-74.

20. Koziol, L.; Valdez, C. A.; Baker, S. E.; Lau, E. Y.; Floyd, W. C., 3rd; Wong, S. E.; Satcher, J. H., Jr.; Lightstone, F. C.; Aines, R. D., Toward a Small Molecule, Biomimetic Carbonic Anhydrase Model: Theoretical and Experimental Investigations of a Panel of Zinc(Ii) Aza-Macrocyclic Catalysts; *Inorg. Chem.* **2012,** *51*, 6803-6812.

21. Satcher, J. H.; Baker, S. E.; Kulik, H. J.; Valdez, C. A.; Krueger, R. L.; Lightstone, F. C.; Aines, R. D., Modeling, Synthesis and Characterization of Zinc Containing Carbonic Anhydrase Active Site Mimics; *Energy Procedia* **2011,** *4*, 2090-2095.

22. Sun, Y.-J.; Zhang, L. Z.; Sun, W.; Cheng, P.; Lin, H.-K.; Yan, S.-P.; Liao, D.-Z.; Jiang, Z.-H.; Shen, P.-W., Kinetics and Mechanism of the Bicarbonate Dehydration of the Half-Sandwich Zinc(II) Complexes [Tpph]Znx ([Tpph] = Hydrotris(3-Phenylpyrazolyl)Borate; X− = Oh−, N3−, Ncs−); *J. Mol. Catal. A: Chem.* **2003,** *198*, 99-106.

23. Kimura, E.; Shiota, T.; Koike, T.; Shiro, M.; Kodama, M., A Zinc(II) Complex of 1,5,9-Triazacyclododecane ([12]Anen^3) as a Model for Carbonic Anhydrase; *J. Am. Chem. Soc.* **1990,** *112*, 5805-5811.

24. Nakata, K.; Shimomura, N.; Shiina, N.; Izumi, M.; Ichikawa, K.; Shiro, M., Kinetic Study of Catalytic CO_2 Hydration by Water-Soluble Model Compound of Carbonic Anhydrase and Anion Inhibition Effect on CO_2 Hydration; *J. Inorg. Biochem.* **2002,** *89*, 255-266.

25. Rowlett, R. S., Structure and Catalytic Mechanism of the Beta-Carbonic Anhydrases; *Biochim. Biophys. Acta* **2010,** *1804*, 362-373.

26. Silverman, D. N.; Vincent, S. H., Proton Transfer in the Catalytic Mechanism of Carbonic Anhydras; *Crit. Rev. Biochem. Mol. Biol.* **1983,** *14*, 207-255.

27. Kulik, H. J.; Wong, S. E.; Baker, S. E.; Valdez, C. A.; Satcher, J. H., Jr.; Aines, R. D.; Lightstone, F. C., Developing an Approach for First-Principles Catalyst Design: Application to Carbon-Capture Catalysis; *Acta Crystallogr., Sect. C: Struct. Chem.* **2014,** *70*, 123-131.

28. Bandeira, N. A.; Garai, S.; Muller, A.; Bo, C., The Mechanism of Co2 Hydration: A Porous Metal Oxide Nanocapsule Catalyst Can Mimic the Biological Carbonic Anhydrase Role; *Chem. Commun. (Cambridge, U. K.)* **2015,** *51*, 15596-15599.

29. Piazzetta, P.; Marino, T.; Russo, N.; Salahub, D. R., Direct Hydrogenation of Carbon Dioxide by an Artificial Reductase Obtained by Substituting Rhodium for Zinc in the Carbonic Anhydrase Catalytic Center. A Mechanistic Study; *ACS Catal.* **2015,** *5*, 5397-5409.

30. Yu, F.; Cangelosi, V. M.; Zastrow, M. L.; Tegoni, M.; Plegaria, J. S.; Tebo, A. G.; Mocny, C. S.; Ruckthong, L.; Qayyum, H.; Pecoraro, V. L., Protein Design: Toward Functional Metalloenzymes; *Chem. Rev.* **2014,** *114*, 3495-3578.

31. Pocker, Y.; Bjorkquist, D. W., Stopped-Flow Studies of Carbon Dioxide Hydration and Bicarbonate Dehydration in Water and Water-D2. Acid-Base and Metal Ion Catalysis; *J. Am. Chem. Soc.* **1977,** *99*, 6537-6543.

32. Brown, R. S.; Curtis, N. J.; Huguet, J., Tris(4,5-Diisopropylimidazol-2-Yl)Phosphine-Zinc(2^+) - a Catalytically Active Model for Carbonic-Anhydrase; *J. Am. Chem. Soc.* **1981,** *103*, 6953-6959.

33. Zhang, X.; van Eldik, R.; Koike, T.; Kimura, E., Kinetics and Mechanism of the Hydration of Carbon Dioxide and Dehydration of Bicarbonate Catalyzed by a Zinc (II) Complex of 1,5,9-Triazacyclododecane as a Model for Carbonic Anhydrase; *Inorg. Chem.* **1993,** *32*, 5749-5755.

34. Zhang, X.; van Eldik, R., A Functional Model for Carbonic Anhydrase: Thermodynamic and Kinetic Study of a Tetraazacyclododecane Complex of Zinc(II); *Inorg. Chem.* **1995,** *34*, 5606-5614.

35. Sun, Y.-J.; Zhang, L. Z.; Cheng, P.; Lin, H.-K.; Yan, S.-P.; Liao, D.-Z.; Jiang, Z.-H.; Shen, P.-W., Dehydration Kinetic Studies of Hco3− Catalyzed by Three Half-Sandwich Nickel(Ii) Complexes in the Presence of Inhibitors NO_2^-, N_3^- and NCS^-; *Inorg. Chem. Commun.* **2004,** *7*, 165-168.

36. Sun, Y.-J.; Zhang, L. Z.; Cheng, P.; Lin, H.-K.; Yan, S.-P.; Liao, D.-Z.; Jiang, Z.-H.; Shen, P.-W., Experimental and Theoretical Studies of the Dehydration Kinetics of Two Inhibitor-Containing Half-Sandwich Cobalt(Ii) Complexes; *J. Mol. Catal. A: Chem.* **2004,** *208*, 83-90.

37. Davy, R., Development of Catalysts for Fast, Energy Efficient Post Combustion Capture of CO_2 into Water; an Alternative to Monoethanolamine (Mea) Solvents; *Energy Procedia* **2009,** *1*, 885-892.

38. Rodionov, V. O.; Presolski, S. I.; Gardinier, S.; Lim, Y. H.; Finn, M. G., Benzimidazole and Related Ligands for Cu-Catalyzed Azide-Alkyne Cycloaddition; *J. Am. Chem. Soc.* **2007,** *129*, 12696-12704.

39. Gibbons, B. H.; Edsall, J. T., Rate of Hydration of Carbon Dioxide and Dehydration of Carbonic Acid at 25°C; *J. Biol. Chem.* **1963,** *238*, 3502-3507.

40. Tu, C. K.; Thomas, H. G.; Wynns, G. C.; Silverman, D. N., Hydrolysis of 4-Nitrophenyl Acetate Catalyzed by Carbonic Anhydrase-III from Bovine Skeletal-Muscle; *J. Biol. Chem.* **1986,** *261*, 100-103.

41. Bräuer, M.; Pérez-Lustres, J. L.; Weston, J.; Anders, E., Quantitative Reactivity Model for the Hydration of Carbon Dioxide by Biomimetic Zinc Complexes⊥; *Inorg. Chem.* **2002,** *41*, 1454-1463.

42. Echizen, T.; Ibrahim, M. M.; Nakata, K.; Izumi, M.; Ichikawa, K.; Shiro, M., Nucleophilic Reaction by Carbonic Anhydrase Model Zinc Compound: Characterization of Intermediates for CO_2 Hydration and Phosphoester Hydrolysis; *J. Inorg. Biochem.* **2004,** *98*, 1347-1360.

43. Han, R., Structural and Spectroscopic Studies on Four-, Five-, and Six-Coordinate Complexes of Zinc, Copper, Nickel, and

Cobalt: Structural Models for the Bicarbonate Intermediate of the Carbonic Anhydrase Catalytic Cycle; *J. Inorg. Biochem.* **1993,** *49*, 105-121.

44. Alzuet, G.; Casella, L.; Perotti, A.; Borrás, J., Acetazolamide Binding to Zinc(II), Cobalt(II) and Copper(II) Model Complexes of Carbonic Anhydrase; *J. Chem. Soc., Dalton Trans.* **1994**, *0*, 2347-2351.

45. Chufán, E. E.; García-granda, S.; Díaz, M. R.; Borrás, J.; Pedregosa, J. C., Several Coordination Modes of 5-Amino-1,3,4-Thiadiazole-2-Sulfonamide (Hats) with Cu(II), Ni(II) and Zn(II): Mimetic Ternary Complexes of Carbonic Anhydrase-Inhibitor; *J. Coord. Chem.* **2001,** *54*, 303-312.

46. Koike, T.; Kimura, E.; Nakamura, I.; Hashimoto, Y.; Shiro, M., The First Anionic Sulfonamide-Binding Zinc(II) Complexes with a Macrocyclic Triamine: Chemical Verification of the Sulfonamide Inhibition of Carbonic Anhydrase; *J. Am. Chem. Soc.* **1992,** *114*, 7338-7345.

47. Lin, Y.-W., Rational Design of Metalloenzymes: From Single to Multiple Active Sites; *Coord. Chem. Rev.* **2017,** *336*, 1-27.

48. Lopez, M.; Vu, H.; Wang, C. K.; Wolf, M. G.; Groenhof, G.; Innocenti, A.; Supuran, C. T.; Poulsen, S. A., Promiscuity of Carbonic Anhydrase Ii. Unexpected Ester Hydrolysis of Carbohydrate-Based Sulfamate Inhibitors; *J. Am. Chem. Soc.* **2011,** *133*, 18452-18462.

49. Williams, R. J. P., Bio-Inorganic Chemistry: Its Conceptual Evolution; *Coord. Chem. Rev.* **1990,** *100*, 573-610.

50. Woolley, P., Models for Metal Ion Function in Carbonic Anhydrase; *Nature (London, U. K.)* **1975,** *258*, 677-682.

51. Di Fiore, A.; Monti, S. M.; Hilvo, M.; Parkkila, S.; Romano, V.; Scaloni, A.; Pedone, C.; Scozzafava, A.; Supuran, C. T.; De Simone, G., Crystal Structure of Human Carbonic Anhydrase Xiii and Its Complex with the Inhibitor Acetazolamide; *Proteins: Struct., Funct., Bioinf.* **2009,** *74*, 164-175.

52. Zastrow, M. L.; Peacock, A. F.; Stuckey, J. A.; Pecoraro, V. L., Hydrolytic Catalysis and Structural Stabilization in a Designed Metalloprotein; *Nat. Chem.* **2011,** *4*, 118-123.

53. Baird, T. T., Jr.; Waheed, A.; Okuyama, T.; Sly, W. S.; Fierke, C. A., Catalysis and Inhibition of Human Carbonic Anhydrase Iv; *Biochemistry* **1997,** *36*, 2669-2678.

54. Bertucci, A.; Innocenti, A.; Zoccola, D.; Scozzafava, A.; Allemand, D.; Tambutte, S.; Supuran, C. T., Carbonic Anhydrase Inhibitors: Inhibition Studies of a Coral Secretory Isoform with Inorganic Anions; *Bioorg. Med. Chem. Lett.* **2009,** *19*, 650-653.

55. Supuran, C. T.; Popescu, A.; Ilisiu, M.; Costandache, A.; Banciu, M. D., Carbonic Anhydrase Inhibitors. Part 36. Inhibition of Isozymes I and Ii with Schiff Bases Derived from Chalkones and Aromatic/Heterocyclic Sulfonamides; *Eur. J. Med. Chem.* **1996,** *31*, 439-447.

56. Rusconi, S.; Innocenti, A.; Vullo, D.; Mastrolorenzo, A.; Scozzafava, A.; Supuran, C. T., Carbonic Anhydrase Inhibitors. Interaction of Isozymes I, II, IV, V, and IX with Phosphates, Carbamoyl Phosphate, and the Phosphonate Antiviral Drug Foscarnet; *Bioorg. Med. Chem. Lett.* **2004,** *14*, 5763-5767.

Graphical Abstract